Ind. J. Pharm. Edu. Res., 2026; 60(4s):s1498-s1513.
https://www.ijper.org

Original Article

Deferoxamine Loaded Nanoemulgel for Enhanced Wound Healing: Formulation Optimization and *in vivo* Evaluation

Abdullah M. Alotaibi[1], Anroop B. Nair, Hiral Shah[3], Bandar Aldhubiab[2], Shery Jacob[4], Rashed M. Almuqbil[2,*], Ahmed S. Alnaim[2], Jigar N. Shah[5]

[1]Department of Pharmaceutical Care, Al-Ahsa Health Cluster, Ministry of Health, Al-Ahsa, SAUDI ARABIA.
[2]Department of Pharmaceutical Sciences, College of Clinical Pharmacy, King Faisal University, Al-Ahsa, SAUDI ARABIA.
[3]Department of Pharmaceutics, Parul College of Pharmacy and Research, Parul University, Ahmedabad, Gujarat, INDIA.
[4]Department of Pharmaceutical Sciences, College of Pharmacy, Gulf Medical University, Ajman, UNITED ARAB EMIRATES.
[5]Department of Pharmaceutics, Institute of Pharmacy, Nirma University, Ahmedabad, Gujarat, INDIA.

ABSTRACT

Background: Chronic wounds remain a major clinical challenge due to impaired angiogenesis, persistent inflammation, and oxidative stress, necessitating advanced therapeutic strategies. The purpose of this research was to design, develop and evaluate deferoxamine loaded nanoemulgel for enhanced topical delivery and wound healing. **Materials and Methods:** Deferoxamine loaded nanoemulsions were formulated by aqueous titration method using oleic acid, Tween 80, and propylene glycol as oil, surfactant, and co-surfactant, respectively. Formulation was optimized using central composite design and characterized for droplet properties. The selected nanoemulsion was subsequently formulated into carbopol based hydrogel system and evaluated for physicochemical properties, release kinetics, skin deposition, skin irritation, and wound healing in rats. **Results:** The selected nanoemulsion had particle size of ~88 nm, low polydispersity (0.39), and high zeta potential (-52 mV), indicating good physical stability. TEM image indicates spherical shape, uniform dispersion and absence of agglomeration of prepared nanoemulsion. Thermodynamic stability data confirm that the nanoemulsion did not exhibit any phase separation or creaming. Deferoxamine nanoemulgel demonstrated suitable physicochemical properties, including acceptable pH (6.12±0.30), high drug content (97.84±2.06%), optimal viscosity (85356±2834 cP), and adequate spreadability (15.88±0.50 cm). *In vitro* release profile revealed sustained deferoxamine release over 12 hr following Korsmeyer-Peppas kinetics (R^2=0.9964), while *ex vivo* studies demonstrated significantly higher (p<0.001) skin deposition compared to control gel. The nanoemulgel was found to be non-irritant and well tolerated. *In vivo* wound healing studies in rats demonstrated significantly enhanced (p<0.0001) wound contraction reaching 100% by day 14, along with improved granulation tissue formation and accelerated re-epithelialization as compared to blank formulation. Histopathological analysis confirmed improved collagen organization and reduced inflammation. **Conclusion:** Overall, the observed results establish that the deferoxamine nanoemulgel is a promising strategy for targeted, sustained, and effective management of wounds.

Keywords: Deferoxamine, Hydrogel, Nanoemulsion, Optimization, Rats, Wound healing.

Correspondence:
Rashed M. Almuqbil
Department of Pharmaceutical Sciences, College of Clinical Pharmacy, King Faisal University, Al-Ahsa-31982, SAUDI ARABIA.
Email: ralmuqbil@kfu.edu.sa

Received: 18-02-2026;
Revised: 06-04-2026;
Accepted: 22-06-2026.

INTRODUCTION

Nearly 10.5 million United States population experiences decline in their quality of life due to chronic wounds, with their management exerting noteworthy economic influence on healthcare.[1] It is projected that chronic wounds will persist as substantial clinical, social, and economic challenge because of the aging population, along with widespread risks of diabetes and obesity worldwide. Chronic wounds are those that have not followed the typical healing process and remain open for duration exceeding one month. Regeneration and tissue repair are highly complex and tightly regulated biological processes initiated immediately following tissue injury. They involve coordinated cascade of molecular and cellular events such as inflammation, cell migration, proliferation, angiogenesis, and extracellular matrix remodeling. In addition, wound healing progresses through distinct phases such as hemostasis, inflammation, proliferation with granulation tissue formation and reepithelialization and eventually tissue remodeling.[2] These events are caused by dynamic mechanisms that involve soluble mediators (including cytokines, chemokines, and growth factors) and various cellular components, such as resident skin cells, peripheral blood mononuclear cells, blood cells, and parenchymal

DOI: 10.5530/ijper.20265633

cells. The improper functioning of the immune system results in persistent inflammation and compromised wound healing, ultimately causing development of chronic or non-healing skin wounds.[3] Besides immune imbalances, delayed healing in chronic wounds can be attributed to low nitric oxide levels and high levels of reactive oxygen species.[4] A crucial element in the perpetuation of chronic inflammation seems to be the excessive infiltration of neutrophils, serving as biomarker for chronic wounds in this cycle.[5] Another contributing factor to delayed wound healing is the dysregulation of matrix metalloproteinases, which leads to compromised epithelialization and is closely linked to the difficulty in healing persistent wounds.[6] Oxidative stress and inflammation stand out as primary factors that have the potential to disrupt this process, serving as major contributors to delayed wound healing.[7] The Fenton reaction occurring in wound induces oxidative stress, leading to overproduction of reactive oxygen species, with iron playing crucial role in facilitating this process.[8] The primary source of the oxidative burst is the activated macrophages and neutrophils recruited to the wound site.[9] The iron-catalyzed formation of reactive oxygen species is suggested as crucial mechanism linked to the accelerated apoptosis in injured tissues, contributing to slow rate of wound healing. The induction of heat shock proteins, combined with the accumulation of inorganic iron in the injured tissues, partially elucidates the induced apoptosis in these areas.[10] The oxidative burden is intensified by wound infection, leading the iron carrier protein lactoferrin to exert powerful bacteriostatic effects by removing iron from bacterial access, thereby controlling potential infections.[11] Iron complexing agents, such as deferoxamine, have been reported to exhibit wound healing benefits in various conditions such as sickle cell ulcers[12] and skin wounds,[13] where they promote neovascularization and enhance the overall wound healing process.

Deferoxamine mesylate (*Desferal*) is the only iron-chelating agent approved by the FDA. It has shown the capacity to improve the healing process of diabetic ulcers by stabilizing hypoxia inducible factor-1 alpha, leading to the promotion of neovascularization and the inhibition of responses to oxidative stress.[14,15] There are sources of concern after parenteral delivery because of the potential adverse effects stemming from its strong iron-lowering properties and comparatively short serum half-life, as well as slow gastrointestinal absorption after oral administration.[16] Despite being non-toxic, deferoxamine has been linked to cataracts, deafness, and local skin reactions including urticaria. Various studies highlighted the increased risk of severe systemic reactions, especially in geriatric patients, associated with the oral consumption of deferoxamine.[17] Methods assessed for delivering deferoxamine for localized effects include topical spray, cream,[18] transfersomes,[19] nanofibers,[20] and various dermal formulations, as well as drug-eluting wound dressings and transdermal patches. Although sustained-release transdermal drug delivery system for deferoxamine has been developed using reverse micellar technologies, the use of plasticizers, emulsifiers, and surfactants poses a potential challenge to the clinical application of this treatment.[16] On the other hand, micro-texturing technology was utilized to enhance the release of deferoxamine to overcome regulatory constraints.[13] However, this approach may be limited by scalability challenges, manufacturing complexity, and variability in drug release profiles.

Nanoemulsions are versatile colloidal drug delivery systems composed of nanosized droplets (20-200 nm) that provide significant advantages in pharmaceutical applications, including enhanced drug solubility, improved physicochemical stability, and increased bioavailability of poorly water-soluble drugs.[21] Their small droplet size and large interfacial surface area facilitate sustained drug release, increase in dermal retention and prolonged duration, improved drug permeation through biological membranes, reduce systemic adverse effects, making them particularly suitable for topical and transdermal delivery.[22] Furthermore, nanoemulsions can be added to gel matrices to produce nanoemulgels, which combine the benefits of traditional gels and nano-sized delivery systems. This hybrid system improves rheological properties, enhances patient compliance, and allows for prolonged residence time at the application site.[23] Nanoemulgel provides sustained therapeutic effects with reduced dosing frequency and enables targeted delivery of agents such as pro-angiogenic compounds to the wound area while decreasing systemic side effects.[24] Given the impaired angiogenesis and persistent inflammation characteristic of chronic wounds, nanoemulgel-based topical delivery of deferoxamine (a hypoxia-inducible factor-1α stabilizer) represents promising approach to enhance vascularization and promote tissue regeneration. Hence, the objective of this study was to design, develop and evaluate the feasibility of deferoxamine loaded nanoemulgel for improving topical wound healing. Oleic acid (oil), Tween 80 (surfactant), and propylene glycol (co-surfactant) were selected based on solubility screening results and nanoemulsions were prepared using aqueous titration. Optimization of nanoemulsion was carried out by central composite design (3-factor 3-level) by assessing the influence of amount of oil (%), S_{mix} (%), and water (%) on nanoemulsion formulation. Optimized drug loaded nanoemulsion was characterized and subsequently formulated into nanoemulgel, evaluated for physicochemical characters, drug release, skin deposition, skin irritation, and wound healing in rats.

MATERIALS AND METHODS

Materials

Deferoxamine mesylate was purchased from Sigma Aldrich, St. Louis, USA. Iron (II) sulphate heptahydrate, oleic acid, and Carbopol 940 were purchased commercially from Sigma Aldrich/ Merck, Darmstadt, Germany. Tween 40, Tween 60, Tween 80, Span 80, propylene glycol, polyethylene glycol 400, and castor

oil were procured from Sisco Research Laboratories Pvt. Ltd., Mumbai, India. Transcutol-P and caproyl 90 were received as gift sample from Gattefosse, Mumbai, India. Olive oil and dil oil were purchased from Yarrow Chem Products, Mumbai, India. Witepsol E 85 was obtained as gratis sample from IOI Oleochemicals, Hamburg, Germany. Ethanol was procured from Ureca stores, Ahmedabad, India. The remaining chemicals were of analytical grade and were used in their received form.

Analysis of Deferoxamine

Deferoxamine in samples was measured with minor modification of the HPLC method reported in the literature.[25] Briefly, the standard stock solutions containing 0.005 M of deferoxamine were prepared by dissolving in Milli Q water (Millipore, Bedford, MA, USA). Similarly, standard stock solutions containing 0.025 M of iron (II) sulphate were prepared. Then the drug-metal ion complexation was done by transferring equal volume of drug and metal ion solutions (1 mL) and the volume was adjusted to 5 mL with 0.1% formic acid to obtain drug/metal ion molar ratio of 1:5. The mixture was sonicated for 5 min and filtered using hydrophilic polyvinylidene difluoride membrane (0.45 µm). The resulting solutions were further diluted with 0.1% formic acid and injected into an Agilent 1260 infinity HPLC (Santa Clara, CA, USA) consisting of C-18 endcapped lichrospher column (Merck, Germany) maintained at 25°C. Formic acid (0.1%) and methanol (95:5 v/v) mixture was used as mobile phase to elute deferoxamine-Fe^{2+} complex with a flow rate of 1 mL/min. The samples were measured at λ_{max} 260 nm, and the observed retention time was 5.827 min.

Screening of Oil, Surfactant, and Co-Surfactant

The phase solubility of deferoxamine in different oils and mixture of surfactants and co-surfactants (S_{mix}) was determined according to the method described previously.[26] The oils assessed were caproyl 90, oleic acid, castor oil, olive oil, dil oil, and witepsol E 85. The surfactants tested were Tween 80, Tween 60, Tween 40, Span 80 and the co-surfactants were propylene glycol, ethanol, polyethylene glycol 400, and transcutol-P. Excess amount of deferoxamine was added to separate glass vial containing the formulation ingredients (10 mL). The system was stirred for 72 hr using orbital shaker (RIS 24 Plus, Remi, Mumbai, India) at room temperature. The obtained blends were then centrifuged at 10,000 rpm (R-83; Remi, Mumbai, India) for 30 min. The resulting supernatant was filtered using syringe filter (0.22 µm; Millipore Corporation, Bedford, MA, USA), diluted with water and subjected to HPLC analysis.

Construction of Pseudo-Ternary Phase Diagram

Phase diagrams were created using the titration technique to calculate the nanoemulsion area as described elsewhere.[27] The selected oil (oleic acid), surfactant (Tween 80) and co-surfactant (propylene glycol) and water were used to create nanoemulsion zone at room temperature. The ratio of surfactant and co-surfactant (S_{mix}) was changed to get three different compositions (1:1, 1:2, and 1:3 w/w). The selected S_{mix} (oleic acid; Tween 80, 1:3) was used to prepare 18 different oil and S_{mix} (1:9 to 2:9) for further study. Phase diagrams were produced utilizing the information gathered by making transparent S_{mix} dispersions with the selected oil ratio and gradually adding the necessary volume of water while stirring continuously. The software (Chemix School 10.00, Bergen, Norway) was used to create the phase diagrams using water, oil, and S_{mix} as the three axes.

Method of Preparation of Nanoemulsion

The deferoxamine loaded nanoemulsions were formulated by the established aqueous titration technique, with the oil, surfactant, and co-surfactant amounts determined from the phase diagram. Deferoxamine mesylate (10%) was added to the mixtures of oil (oleic acid), surfactant-co-surfactant (S_{mix}, Tween 80: propylene glycol, 1:3), and then water was gradually added dropwise. The mixture was mixed and vortexed at room temperature to produce clear and homogenous nanoemulsion.

Central Composite Design (CCD) for Optimization of Nanoemulsion

The CCD was used for the optimization of deferoxamine loaded nanoemulsions. As indicated in Table 1, the dependent variables were particle size (nm), polydispersity index (PDI), and transmittance (%) and the independent variables were the amount of oil (%), S_{mix} (%), and water (%). Design Expert (version 13, Stat-Ease Inc., Minneapolis, USA) was the software utilized to optimize the nanoemulsion. The following quadratic polynomial equation was provided by the software for the 3-factor 3-level:

$$Y=\beta0 + \beta1X1 + \beta2X2 + \beta3X3 + \beta12X1X2 + \beta13X1X3 + \beta23X2X3 + \beta11X12 + \beta22X22 + \beta33X32$$

Where Y is the measured response for each combination of factor levels; β_0 is the intercept; β_1, β_2, and β_3 are linear coefficients; β_{12}, β_{13}, and β_{23} are interaction coefficients; β_{11}, β_{22}, and β_{33} are quadratic coefficients based on experimental data and and X_1, X_2, and X_3 denote the levels of the independent variables.[28] The responses were statistically assessed using ANOVA. Additionally, the best formulation was selected using numerical optimization procedure based on the desirability function.

Characterization of Nanoemulsion Formulations

Particle size, Zeta potential and PDI

The globule size, size distribution, zeta potential, and PDI of prepared nanoemulsions were determined using dynamic light scattering with Horiba Zetasizer (SZ-100, Kyoto, Japan). Samples were 10 times diluted with water and an aliquot from each formulation was taken, loaded into the sample chamber, and the measurement was done in triplicate for each formulation.[29]

Transmittance

A Shimadzu UV-vis spectrophotometer (UV-1800, Tokyo, Japan) was used to spectrophotometrically evaluate the percentage transmittance of the prepared nanoemulsion formulations. Distilled water was used to dilute samples (1 mL) of the formulation 100 times, and transparent cuvettes were used for analysis.

Morphology

The surface morphology (size and shape) of nanoemulsion was determined using JEM 2100 transmission electron microscope (JEOL, Tokyo, Japan) at an acceleration voltage of 100 kV. Aliquot nanoemulsion was taken and dispersed in distilled water. A drop of the dispersion was placed on a copper grid covered with carbon, dyed with phosphotungstic acid, and allowed to dry at room temperature. Photographs were captured at 8000× after this grid had been mounted in the device.

FTIR

Spectra of pure deferoxamine, blank nanoemulsion, and optimized deferoxamine containing nanoemulsion were measured using spectrometer (FT/IR-6100, Jasco, Tokyo, Japan). IR spectra were measured between 400 and 4000 cm^{-1}, and samples were scanned at resolution of 16 cm^{-1}.

Thermodynamic Stability Study

The optimized deferoxamine loaded nanoemulsion was tested using centrifugation, freeze-thaw cycles, and heating-cooling cycles. The samples underwent freeze-thaw treatment (-21°C to 25°C) for 48 hr, while the heating-cooling cycle test was performed at six alternate cycles between -4°C and 45°C for 48 hr. Similarly, nanoemulsions were centrifuged (5000 rpm for 10 min) to perform the centrifugation test.[30]

Formulation of Nanoemulgel

The selected nanoemulsion was modified into hydrogel system using Carbopol as gelling agent. Hydrogel was fabricated by the dispersion method. Precisely weighed amount of carbopol 940 (1% w/w) was dispersed in deionised water (100 mL) overnight to hydrate and to cross-linking of polymer. The required amount of nanoemulsion (equivalent to 200 mg of deferoxamine, ~20 mL) was weighed separately and added to 7.5 g of carbopol solution. The solution was mixed for 1 hr and added triethanolamine slowly to neutralize the mixture to get hydrogel system. Then the total volume of gel was made up to 10 g with carbopol, which resulted in 2% w/w deferoxamine loaded nanoemulgel. Control gel was formulated similarly using deferoxamine (2% w/w).

Characterization of Nanoemulgel

Visual examinations of developed nanoemulgel were done to check for color, homogeneity, and appearance. The pH of the nanoemulgel was measured using digital pH meter (Controller Based pH System 362, Ahmedabad, India). Samples (1 g gel) were mixed with 10 mL of MilliQ water and the electrode was immersed in the formulation to record pH. The amount of deferoxamine in the developed nanoemulgel was assessed by taking 500 mg of gel and dispersing it in the mobile phase (10 mL). After 10 min of vortexing and 15 min of centrifugation at 3000 rpm, the supernatant of mixture was filtered through a syringe filter with a pore size of 0.22 µm and subjected to HPLC analysis.

Spreadability and Viscosity

Spreadability was determined based on the method described earlier.[31] Nanoemulgel (0.5 g) was kept between two glass slides (10 cm × 10 cm), and the initial diameter of the resulting circle was noted. A 200 g weight was then applied and set aside for 1 min in order to spread the gel and the diameter was measured again. The viscosity was measured using DV-I prime viscometer (Brookfield, Middleborough, MA, USA) with spindle code 64 operated at 0.5 rpm at 25°C.

In vitro Release Study

Standard Franz diffusion assembly (Logan Instruments Ltd., Somerset, NJ, USA) was used to measure the release of deferoxamine from nanoemulgel and control gel. The barrier for drug release was dialysis membrane (12 kDa), which was kept between chambers. The upper chamber was filled with formulations

Table 1: Factors used in optimizing deferoxamine nanoemulsion.

Factor	Level used (actual, coded)		
	Low (-1)	Medium (0)	High (+1)
Independent variables (% v/v)			
X1=Oil	3	5	7
X2=S_{mix}	45	55	65
X3=Water	28	40	52
Dependent variables	Targets		
Y1=Particle size (nm)	Minimum		
Y2=Polydispersity Index (PDI)	Minimum		
Y3=Transmittance (%)	Enhance		

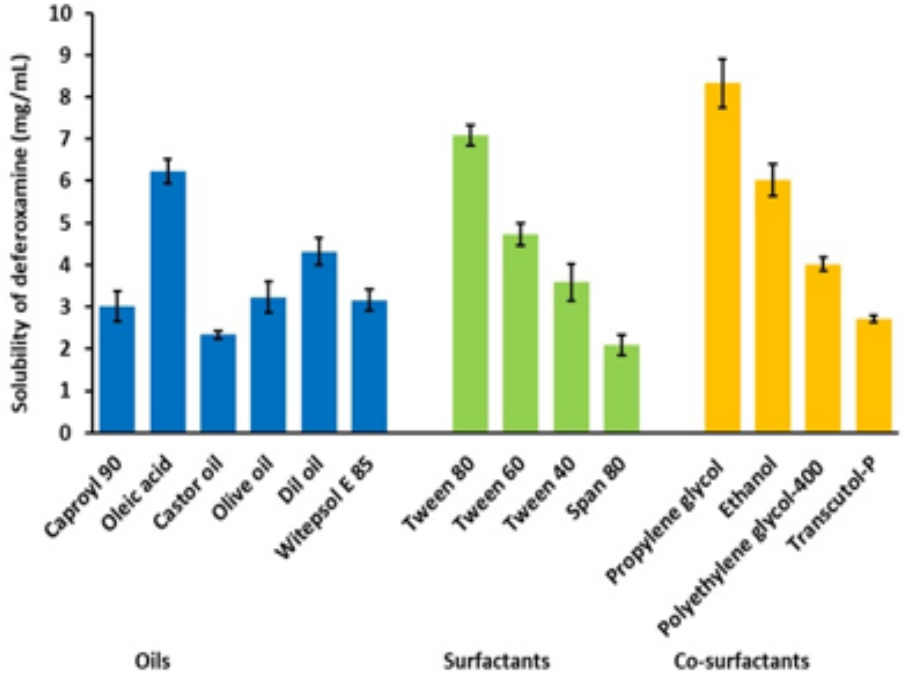

Figure 1: Solubility data of deferoxamine mesylate in various oils, surfactants, and co-surfactants (*n*=6, mean±SD).

(1 g containing 2% w/w deferoxamine of nanoemulgel or control gel), and the region accessible for drug release was 0.74 cm^2. The bottom layer contains phosphate buffered saline (pH=7.4, 5 mL) with Tween 80 (10%), kept at 37±1°C and stirred at 100 rpm. Sample was collected (1 mL) regularly, filtered and analyzed by HPLC. To identify the mechanism of the drug release from the developed nanoemulgel, the cumulative drug release versus time data were fitted and various release kinetics were assessed according to the literature.[32]

Ex vivo Skin Deposition

The deposition of deferoxamine in control gel and nanoemulgel was studied on freshly excised male albino rat skin. The rat skin was cleaned and placed in Franz diffusion apparatus. The receptor medium consisted of 5 mL of phosphate buffered saline and 10% Tween 80, with temperature of 37±1°C. Formulation (500 mg) was kept in the donor compartment, and the quantity of deferoxamine deposited in the active diffusion area of skin was assessed after 12 and 24 hr. The skin was washed five times (with water), wiped using tissue paper, cut into small pieces and soaked in glass vials with methanol (5 mL) for 2 hr with constant sonication.[33] The methanolic solution was filtered using 0.2 µm Millex syringe powered filter (Millipore Corporation, Bedford, MA, USA) and analyzed by HPLC. The extraction procedure was standardized by injecting standard drug solution and the recovery was 82.56±4.71%.

Skin Irritation

Male Wistar rats (200-250 g) were used to assess the skin irritation of the developed nanoemulgel. The University animal ethical committee (KFU-REC-2021-NOV-EA000156) approved the protocol for animal research, which followed international guidelines for the treatment and use of animals. In brief, an electric clipper was used to cut off hair from the rat's dorsal side. Group 1 got received 2.5% sodium dodecyl sulfate, while nanoemulgel and control gel was applied to group 2 and group 3, respectively, and was applied for 24 hr. The Draize cutaneous irritation grading standards were utilized to calculate the test score.

In vivo Study

Before starting the experiment, male Wistar rats weighing approximately 200-250 g were kept at an animal facility for a week. All experimental methods were performed according to the guidelines specified in the university animal ethical approval (KFU-REC-2021-NOV-EA000156), dated November 9, 2021. The eighteen rats were divided into three groups, each with six rats. Using an 8 mm diameter biopsy punch, a circular incision wound was created. Animals in Group 1 (the control group) received no treatment. Group 2 animals received a blank nanoemulgel formulation (200 µL), while group 3 animals received a deferoxamine nanoemulgel (200 µL, or 4 mg of drug). The formulation was applied daily after cleaning the wound area with sterile cotton for 14 days. The wound contraction was calculated according to standard method.[34] On the 14th day of the experiment, the rats were anesthetized for histological analysis,

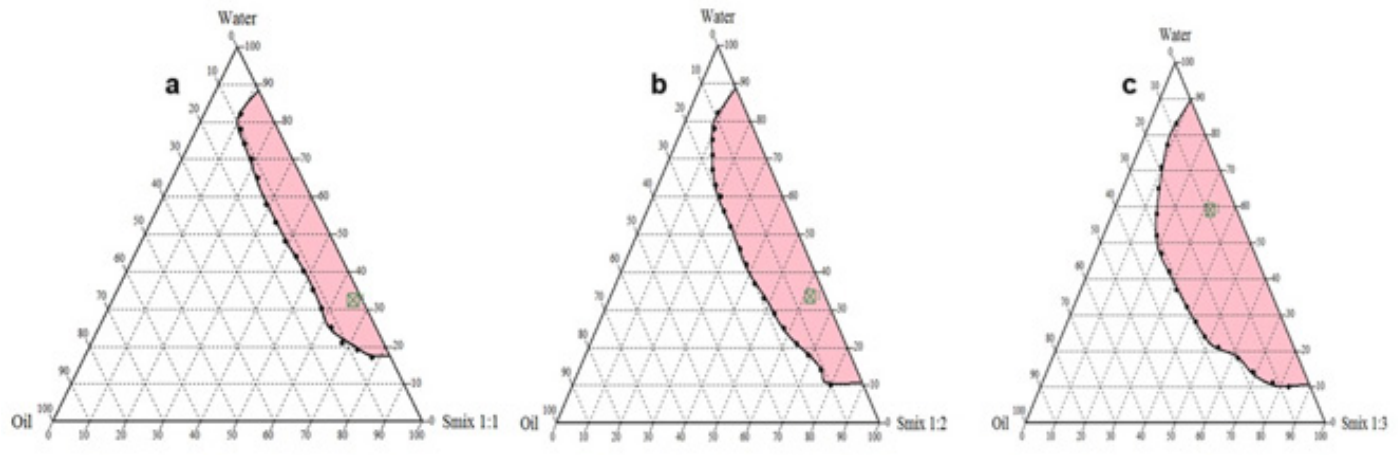

Figure 2: Nanoemulsion area in ternary phase diagrams with different surfactant: co-surfactant ratios of (a) 1:1, (b) 1:2, and (c) 1:3.

Table 2: Estimated and observed values of responses of optimized deferoxamine loaded nanoemulsion.

	Y_1: Particle size (nm)		Y_2: PDI		Y_3: Transmittance (%)	
	Estimated value	Observed value	Estimated value	Observed value	Estimated value	Observed value
Optimized formulation	88.75	88.0	0.390	0.390	89.55	89.26

and the dermis and hypodermis were removed from the incision region using sharp scalpel and trimmer. A 10% formaldehyde solution was used to preserve each tissue sample. The tissue samples were then sectioned using a microtome, encased in paraffin wax, stained with hematoxylin and eosin, and inspected under a microscope.

Stability Study

The test formulation was placed in tightly sealed glass vials for 3 months in refrigerator at 4°C. The formulations were assessed for visual characteristics, deferoxamine concentration, spreading, viscosity, and drug release.

Data Analysis

The results were all displayed as mean±Standard Deviation (SD). GraphPad Prism (version 6) was used to statistically evaluate the data. ANOVA or the student t-test were used, with *p* values less than 0.05 being regarded as significant.

RESULTS AND DISCUSSION

Screening of Oil, Surfactant, and Co-Surfactant

It is crucial to select oils, surfactants, and co-surfactants with the highest solubilizing capability in order to maximize drug loading capacity without causing drug precipitation.[21,35] Figure 1 shows the results of deferoxamine mesylate solubility in different oils, surfactants, and co-surfactants. It has been observed that the highest solubility of deferoxamine in the tested formulation components was found in oleic acid (6.23±0.29 mg/mL), Tween 80 (7.09±0.25 mg/mL), and propylene glycol (8.33±0.58 mg/mL) among the oils, surfactant, and co-surfactant, respectively. Consequently, these ingredients were chosen to develop nanoemulsion preparation. Oleic acid, also known as octadec-9-enoic acid, is a common oil phase used in emulsion systems that helps to improve the skin permeability and can solubilize lipophilic drugs along with its capacity to form microemulsion.[36] It has been reported that certain structural characteristics of oleic acid produce extremely high fluidity, which would serve as the core of nanosystems in the form of liquid droplets.[37] Furthermore, this monounsaturated fatty acid is often used in pharmaceutical formulations due to its high biocompatibility.[38] The high antioxidant content in oleic acid helps in the defense of body against the effects of free radicals, enhances the integrity of cell membranes, and supports the repair of damaged cells and tissues.[39]

The role of surfactant and co-surfactant in nanoemulsion is utmost important as they serve as emulsifier and lower the interfacial tension (at oil-aqueous interphase), which in turn improves the solubility and stability of the nanoemulsion.[40] The non-ionic surfactant, Tween 80, could be suitable choice as it provides numerous benefits like low-toxicity and non irritation and is ideal for formulations aimed for skin delivery.[41] In addition, a stable oil in water (o/w) type nanoemulsion can be produced using Tween 80 with HLB value of 15.[35] It has been described that the combination of oleic acid and Tween 80 can produce ideal nanoemulsion structure owing to the physicochemical features they possess.[37]

The specific role of co-surfactants in nanoemulsion is to support the surfactant in producing small size droplets and increase the

stability of the product. The co-surfactant, propylene glycol has been widely used in nanoemulsions as it can increase interfacial fluidity by integrating into the surfactant layer at the interface, thereby facilitating the formation of nanosized droplets and improving thermodynamic stability of the formulation.[42] Additionally, propylene glycol is widely preferred in skin formulations as they enhance the drug permeation by disturbing the stratum corneum lipids.[43] This chemical is also used as plasticizer in buccal films.[44]

Pseudo-Ternary Phase Diagram

Phase diagrams are helpful tools for identifying the number and kind of phases in a system, their weight percentages, and their composition at specific temperature and system composition.[45] The binodal curve in the phase diagram separates into a transparent nanoemulsion zone and the remaining area indicating turbid and convection emulsion. To determine the range of the nanoemulsion zone, the pseudo-ternary phase diagrams were built using visual observation of the transparent area. The charts were prepared separately for each surfactant to the co-surfactant ratio to identify the o/w nanoemulsion areas for further optimizing the nanoemulsion preparation. Figure 2 represents the phase diagrams of formulation composed of oil (oleic acid) and S_{mix} (Tween 80: propylene glycol in three specific ratios of 1: 1, 1: 2, and 1: 3) dispersed in water at room temperature. Figure 2a indicates certain nanoemulsion region when the ratio was 1:1, indicating the composition is capable to produce emulsion. However, it is always better to use lesser content of surfactant, which may cause skin irritation. Therefore, it was decided to raise the co-surfactant concentration and measure the nanoemulsion area. It was seen in Figure 2b that the nanoemulsion area increases when the surfactant, co-surfactant ratio was changed to 1:2. In another attempt, the surfactant-co-surfactant ratio was increased to 1:3, which further strengthened the nanoemulsion area (Figure 2c) when compared to surfactant-co-surfactant ratio of 1:2. This increase in nanoemulsion area with higher co-surfactant content could be because of more decrease in interfacial tension and higher interfacial layer flexibility, which promote spontaneous curving and the generation of smaller droplets.[42] It is also known that increasing the propylene glycol content in nanoemulsion may also improve the skin penetration of drugs.[43] Therefore, the ideal ratio to use in the nanoemulsion formulation was determined to be 1:3 (w/w) of surfactant to co-surfactant.

CCD for Optimization of Nanoemulsion

When compared to the Box-Behnken design, CCD is preferred because it offers ideas for two more values, +a and -a, which are included within the design criteria for rotatability.[46] Box-Behnken design only recommends formulations with low, mid, and high values for independent variables.[46] After selecting the region of nanoemulsion from the pseudo-ternary phase diagram (Figure 2c), 20 experimental runs (N1-N20) were produced using CCD to find out the best formulation composition for nanoemulsion loaded with deferoxamine. The particle size, PDI, and transmittance were assessed for the 20 designed batches.

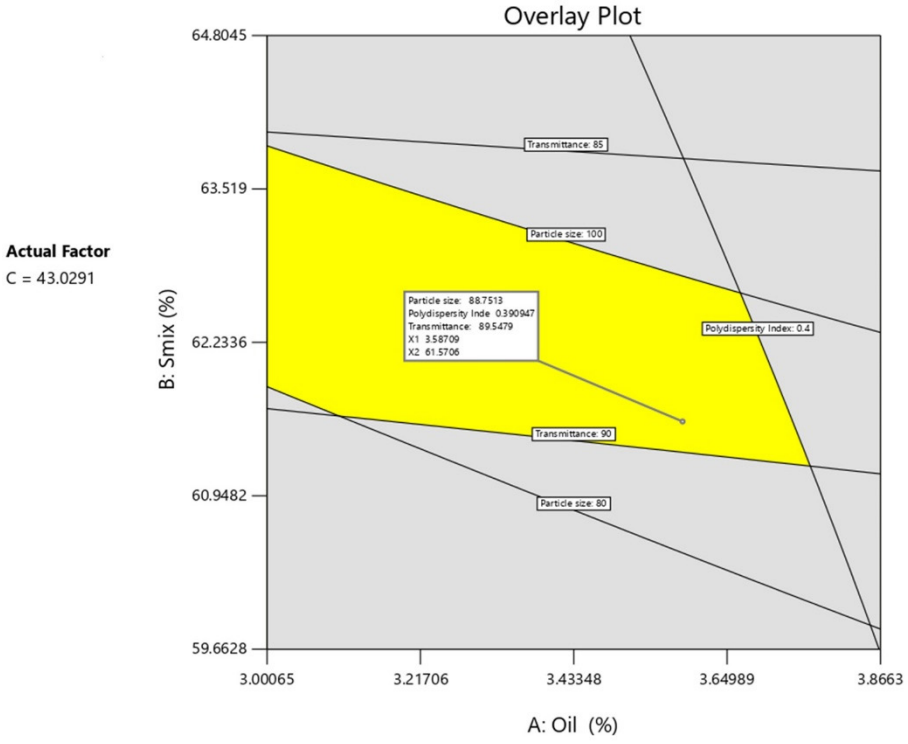

Figure 3: Overlay plot for the selection of best deferoxamine loaded nanoemulsion using design space.

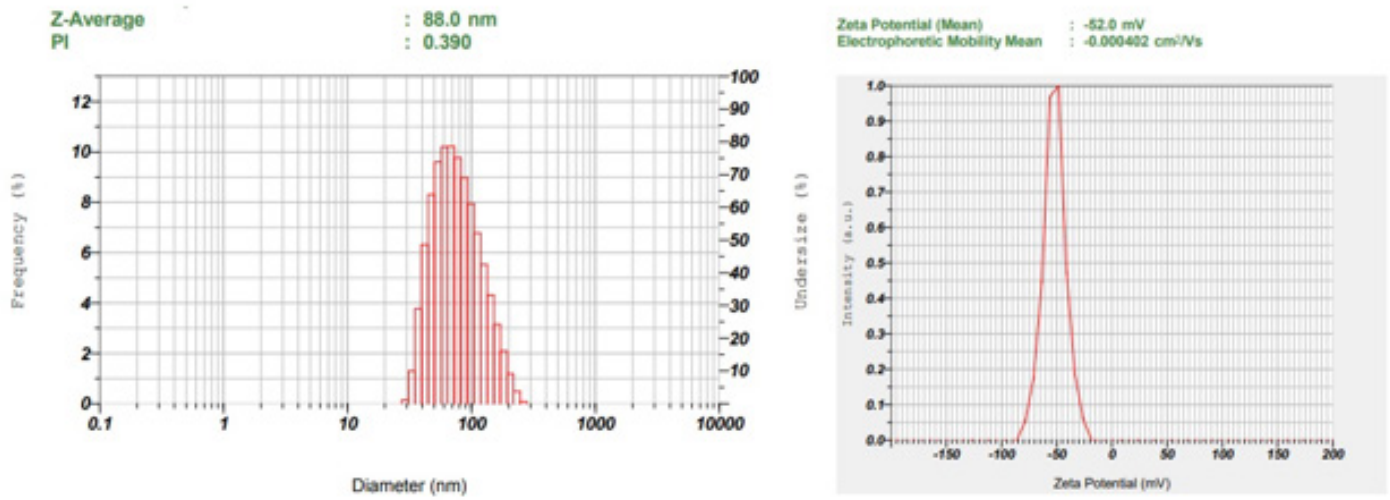

Figure 4: Particle size (a) and zeta potential (b) of optimized deferoxamine loaded nanoemulsion.

Effect on Particle Size

The particle size is one of the most critical elements influencing the physicochemical properties/quality, stability, and efficacy of nanoemulsions.[47] Additionally, the size of the particles is crucial in improving the efficacy of drugs when applied topically, as the small vesicles increase the skin permeation. The influence of input variables (X_1, X_2, and X_3) on the particle size (Y_1) was represented by the following equation:

Y1 (Particle size)=+85.84+12.71X1+19.87X2-59.74X3+4.01X1 X2+1.27X1X3-20.99X2X3-15.22X12+54.08X22+26.07X32

The model is significant (p<0.05), according to its F-value of 2864.88. The model appears to be fit based on the lack of fit F-value of 3.75. The adjusted R^2 (0.9993) and the projected R^2 value (0.9976) are reasonably close. A sufficient signal is indicated by the observed precision (167.38), which is more than 4. It was noticed from the equation that the increase in oil (X_1) and S_{mix} (X_2) will lead to larger particle size while for water (X_3) indicates decrease in the particle size on increasing its amount. The effects of three input factors on particle size are highlighted by means of 3D response surface plots, contour plots, linear correlation between actual and predicted values, and associated residual plots. The red portions in these plots indicate the greatest particle size values, while the yellow, green, and blue areas indicate progressively smaller values. The figure clearly demonstrates direct relation among oil or S_{mix} concentration on the particle size of the nanoemulsion formed. It is evident that the particle size in experimental batches (N1-N20) varied widely between 23 nm (N11) and 275 nm (N2), indicating the influence of input variables on this response. The effect of X_1 is evident in batches N10 and N12, where raising oil amount (3 to 7%), even as retaining other factors same, there was sizeable increase in particle size (Y_1). This is because the higher quantity of oil can lead to rise in emulsion particle size, as documented in an earlier study with oleic acid.[48] Similarly, in case of N15 and N17, where increasing the X_2 amount, while keeping other factors the same, there was significant increase in particle size. It was also observed that after certain point, further increase in S_{mix} concentration resulted in significant increase in droplet size. It is probably due to excess surfactant formed aggregates in the continuous phase with reduced amount of surfactant available to cover the oil phase could have lead to droplet aggregation and increase in droplet size.[48] On the other hand, comparison of N3 and N5 indicates decrease in particle size when the amount of water was increased. This is because the phase inversion process where conversion of phase leads to state of minimal interfacial tension and produce small droplet size.[49]

Effect on PDI

The PDI value indicates the heterogeneity of size distribution of particles and the stability of formulations.[50] This index value in the dispersion ranges between 0 and 1, with values closer to 0 indicating narrow droplet size distribution, while values near 1 indicate polydisperse system. A homogeneous system signifies greater efficacy, where steady drug release and higher bio-availability are observed. The influence of input variables (X_1, X_2, and X_3) on the PDI (Y_2) was represented by the following equation:

Y2 (PDI)=+0.4537+0.0353X1+0.0277X2-0.1179X3+0.0526X1X 2+0.0274X1X3+0.0204X2X3-0.0297X12+0.0293X22+0.0288X32

The model is significant (p<0.05), according to its F-value of 32.49. The model appears to be fit based on the lack of fit F-value of 1.75. The adjusted R^2 (0. 9372) and the projected R^2 value (0. 8145) are moderately close. A sufficient signal is indicated by the observed precision (19.637), which is more than 4. It is observed that with increase in the amount of oil (X_1) and S_{mix} (X_2) will lead to higher PDI (Y_2), while decrease in Y_2 occurs with increase

in water content (X_3). The effects of three input factors on PDI are highlighted by means of 3D response surface plots, contour plots, linear correlation between actual and predicted values, and associated residual plots. The figure clearly demonstrate direct relation between the oil or S_{mix} content and the PDI of the nanoemulsion formed. It is evident that the PDI in experimental batches (N1-N20) varied between 0.302 (N10) and 0.734 (N6), indicating the influence of input variables on this response. The variation in Y_2 was noticed in batches N10 (0.302) and N12 (0.568) with change in X_1 content, which may be because of the increase in viscosity of the formulation, though it has to be examined. Similarly, the effect of X_2 on Y_2 was evident in batches N5 (0.311) and N12 (0.568), which is likely due to the stability of nanoemulsion being affected with increase in S_{mix} as reported elsewhere.[51] However, the increase in water content in the system decreases the Y_2 value as evidenced in N3 (0.554) and N5 (0.311), which could be due to better dispersion of oil in the aqueous phase.

Effect on Transmittance

Transmittance is an important quality control parameter for nanoemulsion, which indicates the visual clarity, stability and uniformity in droplet size. In general, the % transmittance of nanoemulsion near 100% signifies the formulations were clear, transparent and capable of transmitting light across the nanoscale size range.[52] The influence of input variables (X_1, X_2, and X_3) on the % transmittance (Y_3) was represented by the following equation:

$$Y3\ (\%\ Transmittance) = +90.89 - 3.08X1 - 0.9271X2 + 12.95X3 + 1.57X1X2 - 0.8450X1X3 + 3.46X2X3 + 1.24X12 - 13.02X22 - 7.42X32$$

The model is significant ($p<0.05$), according to its F-value of 635.25. The model appears to be fit based on the lack of fit F-value of 3.17. The adjusted R^2 (0. 9967) and the projected R^2 value (0. 9891) are reasonably close. A sufficient signal is indicated by the observed precision (19.637), which is more than 4. It was observed that the increase in the amount of oil and S_{mix} will lead to decrease in % transmittance, while increase in the % transmittance with increase in water content. The effects of three input factors on % transmittance are highlighted by means of 3D response surface plots, contour plots, linear correlation between actual and predicted values, and associated residual plots. The figure clearly demonstrate negative relation between the oil or S_{mix} content and the % transmittance of the nanoemulsion formed. It is evident that the % transmittance in experimental batches (N1-N20) varied between 48% (N6) and 98% (N11), indicating the influence of input variables on this response. The variation in Y_3 was much more evident in batches N18 (89%) and N5 (76%) with change in X_1 content, probably because of oil concentration

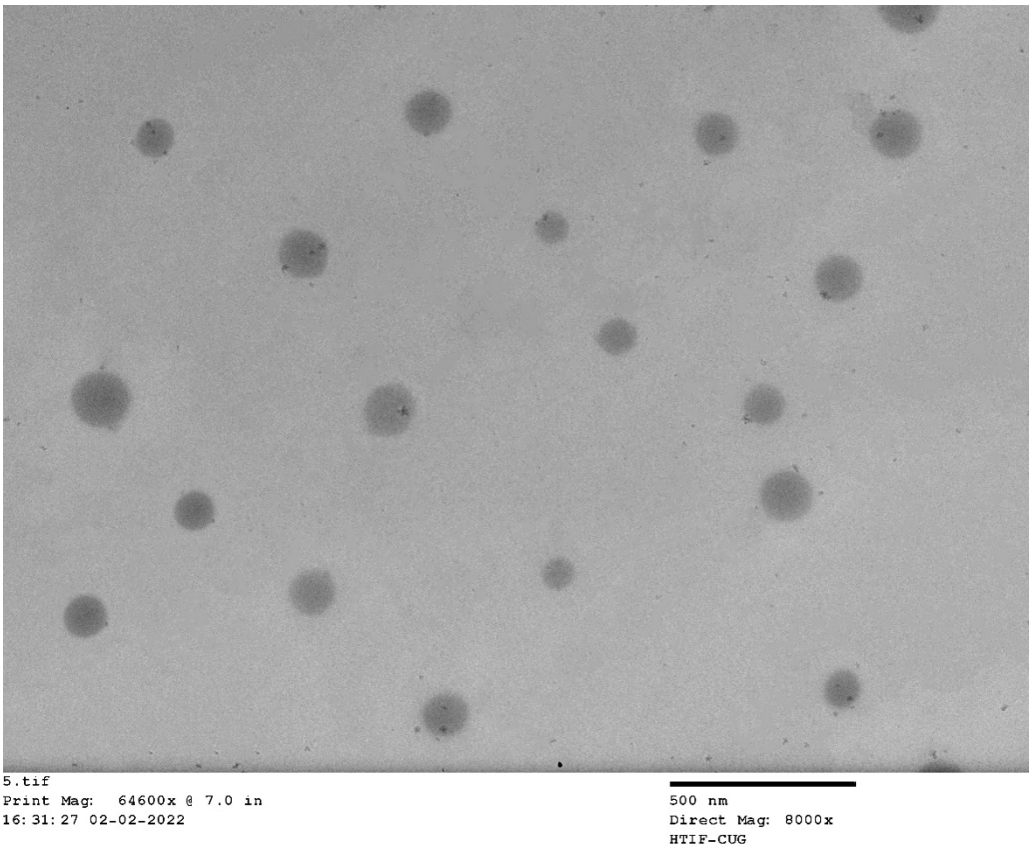

Figure 5: Transmission electron microscopy of optimized deferoxamine loaded nanoemulsion. The scale bar reprfsents 500 nm.

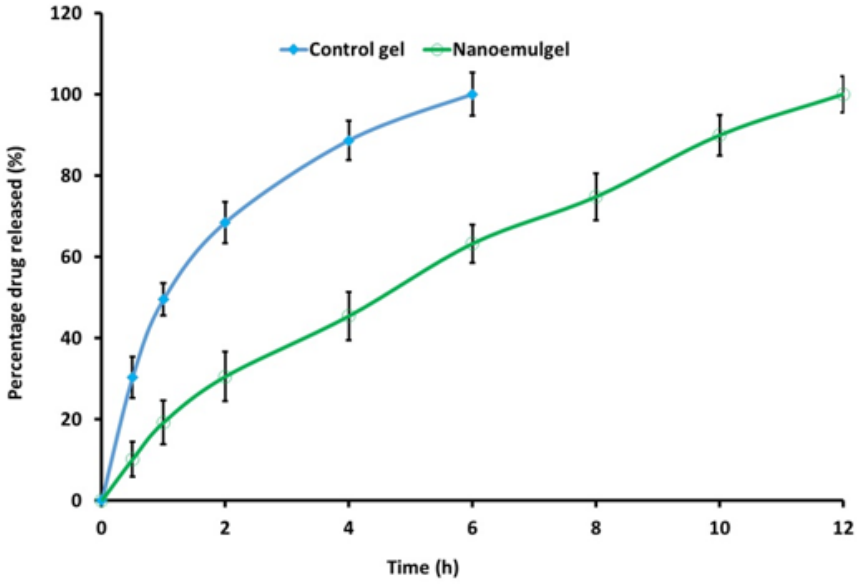

Figure 6: *In vitro* release study of deferoxamine from control (2% w/w deferoxamine gel) and nanoemulgel. Results are expressed as the mean±SD of six experiments.

Table 3: Amount of deferoxamine retained in rat skin at different time intervals from the control gel and nanoemulgel.

	After 12 hr	After 24 hr
Control gel	0.09±0.002 mg/cm^2	0.53 ±0.02 mg/cm^2
Nanoemulgel	2.81±0.31 mg/cm^2	4.72±0.88 mg/cm^2

Results are expressed as the Mean±SD of six experiments.

increases, resulting in increase in droplet size, which leads to greater light scattering and corresponding decrease in % transmittance.[51] Similarly, the effect of X_2 on Y_3 was evident in batches N15 (67%) and N17 (56%), which may be due to increase in Smix concentration beyond ideal ratio resulted in increased coalescence leads to larger particle size and less transparent microemulsion phase.[53] However, the increase in water content in the system increases the Y_2 value as evidenced in N3 (59%) and N5 (76). This could be due to reduction in the size of oil droplets dispersed within the water phase, which leads to small droplet size, results in less scattering of light and more transparent or translucent appearance.[52]

Optimization and Point Prediction

The optimized batch of deferoxamine nanoemulsion was chosen based on the criteria of achieving the best response in particle size, PDI, and transmittance using the graphical point prediction optimization approach of design expert software. Overlay plot on specific focus area for the selection of optimized batch was presented in Figure 3. The composition of the optimized formulation based on design space contains oleic oil (3.51%), S_{mix} (61.81%) and water (42.64%) and was prepared and evaluated. Table 2 shows the estimated and observed values of the selected nanoemulsion. The findings demonstrate that the observed values matched the predictions, and the difference between the estimated and observed values for transmittance, PDI, and particle size was found to be insignificant (p>0.05). Consequently, it was concluded that the derived mathematical equation can accurately predict transmittance, PDI, and particle size.

Evaluation of Optimized Formulation

Particle Size, PDI and Zeta Potential

The droplet size of nanoemulsion plays important role in enhancing wound closure following topical delivery.[23] The droplet size of optimized formulation was ~88 nm, as shown in Figure 4. This allows for close contact with the stratum corneum, which enhances drug penetration and high therapeutic efficacy in wound healing.[54] The PDI value of the developed formulation was 0.390, suggesting homogeneity and uniformity of the nanoemulsion. The zeta potential is crucial for stability because it shows the electrostatic charge on nanostructures, which produces repulsive energy barrier that prevents particle aggregation.[37] It has been described that the zeta potential value higher than ±30 mV implies that the developed nanoemulsion is stable.[55] The observed zeta potential of prepared nanoemulsion was -52 mV (Figure 4), signifying higher stability. The negative value observed here could be due to the spontaneous formation of negative charge at the water-hydrophobic interface when the oil/S_{mix} comes into contact with water, as reported previously.[37]

Morphology

High-resolution electron microscopy is frequently used to analyze the morphology of nanoemulsions, providing vital information about the size and shape of the droplets as well as stability assessment.[56] The shape and dimensions of the optimized

nanoemulsion were recorded and presented in Figure 5. The droplets in the nanoemulsion seem black while the surroundings are light. The image here shows distinct droplets that are spherical, nanometers in size (~100 nm), uniformly distributed, and appear to be distinct without agglomeration. Moreover, the particle size was consistent with the outcomes of zetasizer-based droplet size data.

FTIR

In preformulation studies, FTIR is utilized to determine the stability of the drug in the final formulation and to identify potential drug-excipient incompatibilities. The formulation excipients may interact with the active, resulting in molecular changes that may influence the formulation stability. The FTIR spectra of deferoxamine show distinctive absorption peaks related to its hydroxamic acid and amide functionalities. Prominent absorption bands observed between 3536.81- 3116.40 cm^{-1} are due to the overlap of O-H and N-H stretching vibrations, implying the existence of hydroxamic acid groups and amide linkages, together with strong intermolecular hydrogen bonding. The peak at 2931.27 cm^{-1} corresponds to the asymmetric stretching of aliphatic C-H bonds in methylene (-CH_2) groups. A prominent absorption band at 1631.48 cm^{-1} is attributed to the amide I band, exhibiting C=O stretching vibration of the hydroxamic carbonyl group, hence confirming the preservation of the amide functionality. The band detected at 1565.92 cm^{-1} corresponds to the amide II vibration, resulting from N-H bending in conjunction with C-N stretching. The signal at 1461.78 cm^{-1} is

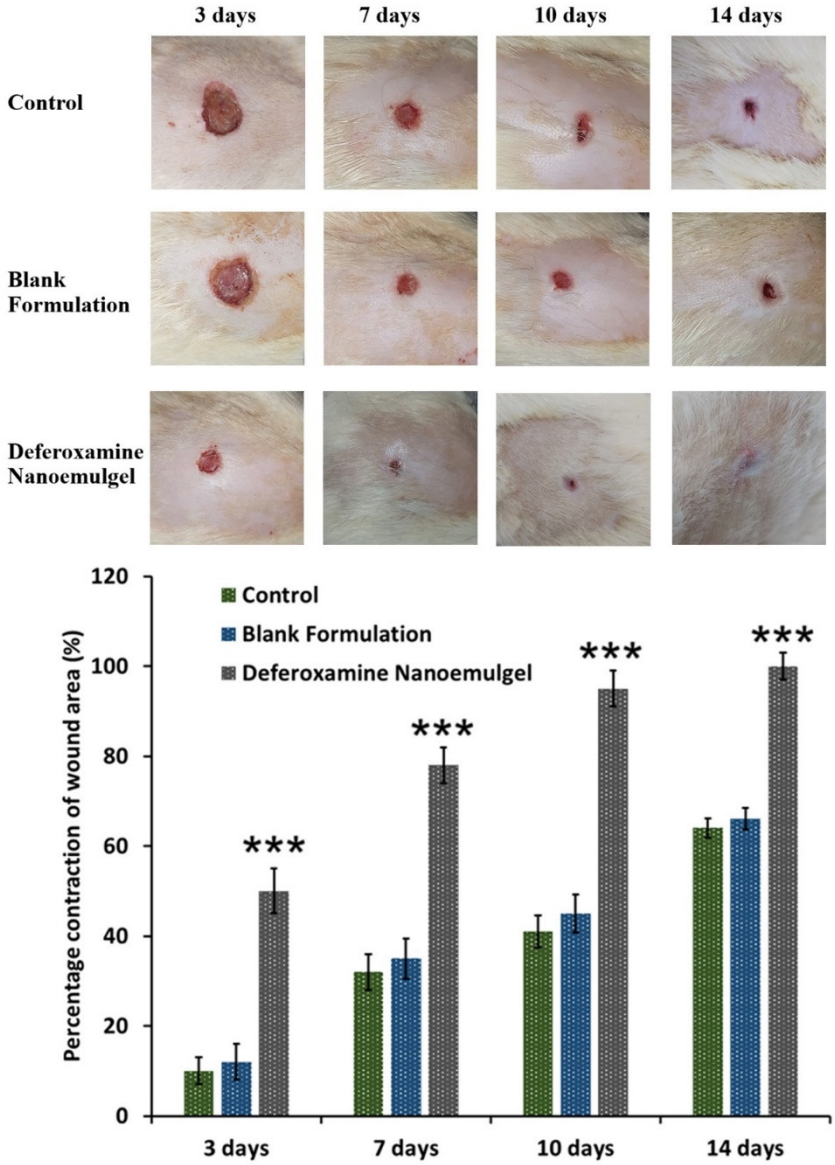

Figure 7: Upper panel: Representative images of wound areas in control, blank formulation, and deferoxamine nanoemulgel from day 0 to day 14 after wound injury. Lower panel: Percentage contraction of wound area. Results are expressed as the mean±SD of six experiments.
*** $p<0.0001$ compared to blank formulation and control on the same day.

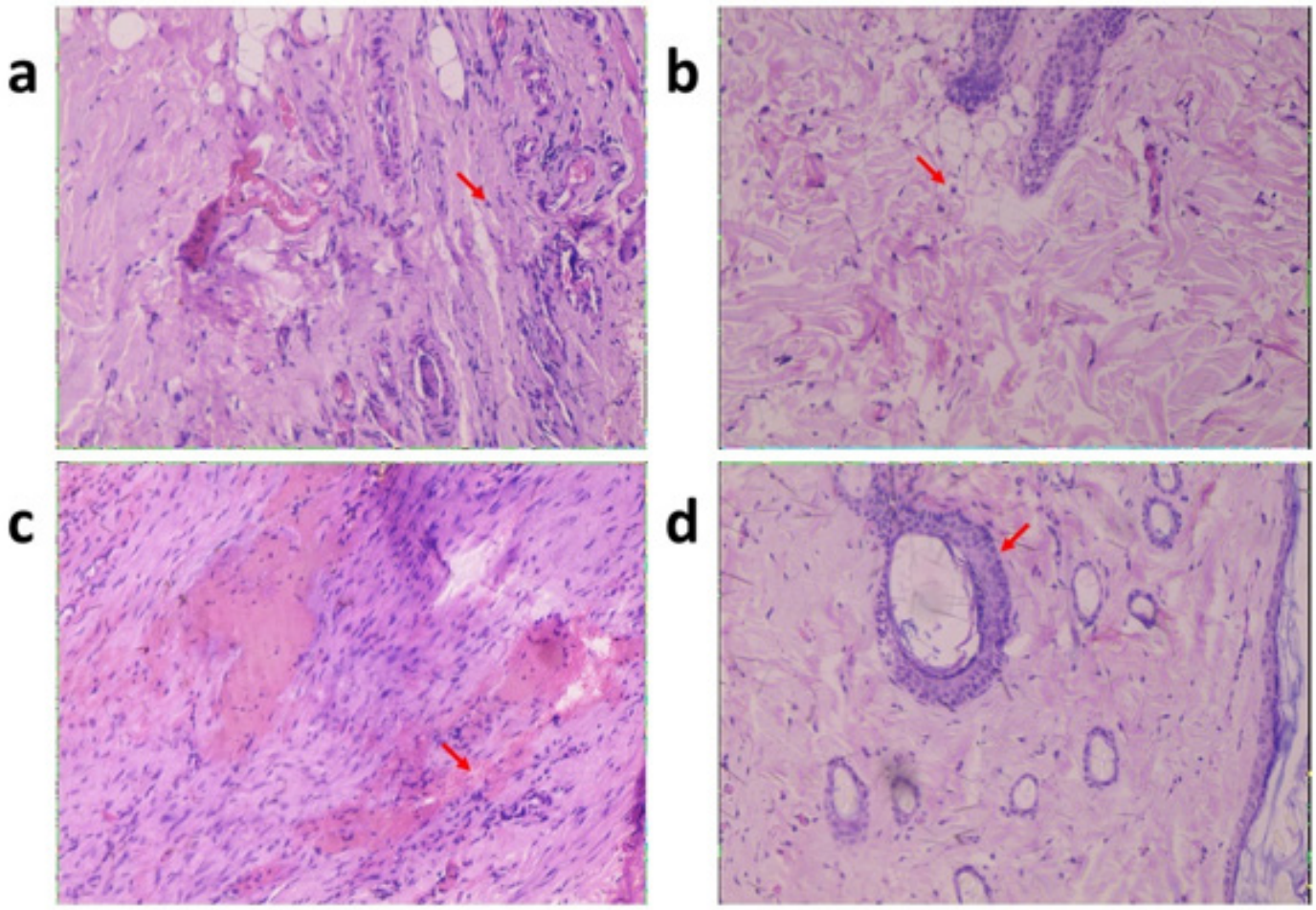

Figure 8: Representative photomicrographs of the rat skin tissues stained with hematoxylin and eosin (40× magnification) at day 14. (a) control group, (b) blank formulation treated, (c) deferoxamine nanoemulgel treated and (d) freshly cut wound.

ascribed to CH_2 bending vibrations of the aliphatic chain. The absorption band at 1203.36 cm^{-1} is attributed to C-N stretching (amide III band), whereas the peak at 1052.94 cm^{-1} belongs to N-O stretching vibration of the hydroxamic acid group, a diagnostic trait essential for iron chelation.[20]

The FTIR spectrum of the deferoxamine loaded nanoemulsion exhibited prominent absorption band at 3486.67 cm^{-1} (O-H and N-H stretching vibrations), 2931.27 cm^{-1} (aliphatic C-H stretching), 1627.63 cm^{-1} (C=O stretching), 1461.78 cm^{-1} (CH_2 bending vibration), 1253.5 cm^{-1} (C-N stretching), 1079.94 cm^{-1} (N-O stretching), hence confirming successful incorporation of deferoxamine within the nanoemulsion system. Minor deviations in peak placements and changes in intensity were noted in the formulation spectrum. These variations could relate to hydrogen bonding interactions, physical encapsulation of the drug within the nanoemulsion matrix, overlap of excipient peaks, and alterations in molecular arrangement. In addition, peaks at 1353.78, 944.94, 883.24, and 694.24 cm^{-1} are likely associated with excipients and structural vibrations of the formulation components, which are also observed in the blank formulation. The presence of all major peaks of deferoxamine in the nanoemulsion spectrum suggests compatibility between the drug and formulation components used, indicating the absence of significant chemical interaction or degradation during formulation.

Thermodynamic Stability Study

Emulsion stability is normally evaluated under stress conditions (temperature as well as centrifugation). Centrifugal techniques are often employed in formulation development to induce and accelerate instability caused by gravity. It is accepted that when an emulsion is centrifuged, the dissociation of the dispersed phase caused by creaming or coalescence can be utilized to quickly predict shelf life under conventional storage conditions.[57] The findings of this investigation reveal that the optimized nanoemulsion did not exhibit any phase separation or creaming following the heating-cooling cycle, freeze-thaw cycles, or centrifugation. Indeed, the favorable results indicate that the emulsion is sufficiently stable.

Characterization of Nanoemulgel

Despite being in the nano-size range, the low viscosity of optimized nanoemulsion formulation makes it difficult to apply

topically for cutaneous use. Hence, the optimized nanoemulsion was modified into hydrogel system with desired consistency using carbopol 940, an excellent rheology modifier that forms clear gel to improve the formulation retention on topical application.[58] The developed nanoemulgel was white, homogeneous viscous preparation with smooth appearance and absence of phase separation. The observed pH of prepared nanoemulgel was 6.12±0.30, which is regarded as acceptable and is not likely to cause any skin irritations when applied.[59] The drug content in the formulation was high (97.84±2.06%), demonstrating uniform dispersion of deferoxamine within the nanoemulgel system.

Spreadability and Viscosity

The spreadability of formulation is one of the most crucial factors to consider when developing topical gels designed for skin application as it indicates the consistency and ease of application that helps to achieve precise dosage distribution.[60] In the current study, the initial diameter of the nanoemulgel measured was 5.22±0.35 cm. However, upon the application of the weight, the diameter increased to 15.88±0.50 cm, indicating adequate spreadability for topical application. The viscosity and spreadability of nanoemulgel are interrelated and influence the performance of the product. Indeed, the viscosity of the formulation can influence spreadability, drug release and permeation when applied topically.[24] The measured viscosity of gel (85356±2834 cP) indicates suitable for topical application and was comparable with earlier data.[61]

In vitro Release Study

Drug release data are essential for evaluating the clinical effectiveness of topical products as they simulate the presence of drugs at the target location.[28] This study ensures the developed formulations homogeneity, potency, and compatibility, while also assists in predicting *in vivo* behavior.[62] The deferoxamine release of nanoemulgel and control is presented in Figure 6. The tested formulations showed two different release characteristics. At all time points, the drug release was slow and steady in nanoemulgel when compared to the control gel. The percentage of drug release in the initial hour was significantly lower (10.19%, $p<0.0001$) in the nanoemulgel than in the control gel (49.51%). It is also evident that the drug release was complete in both formulations, however, the nanoemulgel showed relatively longer release profile (12 hr) than the control gel (6 hr). In fact, the sustained release observed here with nanoemulgel is beneficial for topical wound healing as it prolongs the drug presence at the wound site, which in turn reduces the dosing frequency. The slow release by nanoemulgel compared to the control may be attributed its dual-phase structure, which contains emulsion distributed inside polymeric gel matrix and applies extra mass transfer barrier to drug transport.[63] Assessment of the release data of deferoxamine from the nanoemulgel showed the best fit to the Korsmeyer-Peppas model, as indicated by the high correlation coefficient (R^2=0.9964). The release exponent (n=0.6992) indicates non-Fickian (anomalous) transport mechanism wherein drug release is controlled by combination of diffusion and polymer relaxation processes rather than only Fickian diffusion. Furthermore, the drug release patterns of nanoemulgel and control gel were compared using the similarity (f_2) and dissimilarity (f_1) factors. In fact, the data (f_1=50 and f_2=25) demonstrate that the two formulations had distinct release characteristics. Overall, these findings support the comparatively delayed deferoxamine release from nanoemulgel.

Ex vivo Skin Deposition

Effective topical wound therapy needs sufficient drug retention within the epidermal layers because the local drug availability directly affects therapeutic outcomes.[64] An extended formulation retention at the application site is ideal for better pharmacological activity and greater healing efficacy of deferoxamine, which promotes wound healing by stabilizing hypoxia-inducible pathways and improving vascularization.[14] Therefore, the skin deposition of the developed nanoemulgel was assessed, and the results are presented in Table 3. The results showed significant amount of deferoxamine deposition ($p<0.001$) in the skin layers at both time points in comparison to the control gel. It is also noticed that the drug deposition in nanoemulgel increased significantly ($p<0.05$) from 12 hr to 24 hr and was ~30 and ~9 fold higher than control, respectively. The higher deposition observed with the nanoemulgel could be due to the synergistic effects of the nanoemulsion and the carbopol gel matrix. Overall, the observed greater deferoxamine skin deposition from the nanoemulgel underscores the developed formulation's prospective as a topical delivery strategy for better wound healing outcomes.

Skin Irritation

Skin safety is critical to the safe clinical application of topical products. The skin irritancy test was conducted to detect potential cutaneous reactions of the developed nanoemulgel. A higher irritancy index was noticed with the standard irritant (6.54±1.38), while the values of nanoemulgel (0.98±0.65) and control gel (0.68±0.36) were considerably lower. Moreover, rat skin showed no sign of erythema, edema or inflammation with nanoemulgel or control gel when compared to the standard irritant. This finding demonstrates that the developed nanoemulgel is safe to use topically and is well tolerated.

In vivo Study

Photographs were used for macroscopic examination in order to monitor wound healing. Representative photographs of the wound area in different groups (control, blank formulation and deferoxamine nanoemulgel) are displayed in Figure 7 (upper panel). By day 3, the deferoxamine nanoemulgel treated group had softer thrombus formation, less inflammation, and no exudate, while the control and blank formulation groups had hardened thrombus, swelling, and discharge. In addition, rats treated with

the drug loaded nanoemulgel demonstrated accelerated wound healing, as evidenced by enhanced wound contraction from day 3 to day 14 compared to both control and blank formulation groups. Interestingly, the nanoemulgel treated group developed reddish granulation tissue by day 3. The observed percentage of wound contraction in all groups is presented in Figure 7 (lower panel). The percentage of wound contraction increased in all groups, however, wound healing was significantly higher ($p<0.0001$) in the deferoxamine nanoemulgel group than in the control and blank formulation groups. In deferoxamine nanoemulgel treated group, 50% wound contraction was seen at day 3, which progressively increased to 78%, 95% and 100% by day 7, 10 and 14, respectively. However, the control and blank groups showed 64% and 66% wound closure by day 14. Overall, these findings indicate the improved wound healing efficacy of the developed nanoemulgel formulation.

Histopathological analysis is considered as an essential technique for evaluating wound healing as it provides in-depth microscopic insights into the tissue regeneration process.[65] The photomicrographs of rat tissue sections of different groups are presented in Figure 8. The red arrow shown in Figures 8a and 8b indicates the presence of mononuclear inflammatory cell infiltration in the control and blank formulation treated groups. However, Figure 8c indicates advanced re-epithelialization, vascular structural repair, and well-organized collagen deposition suggesting almost complete tissue regeneration with the deferoxamine nanoemulgel treated group. The existence of ulceration along with higher number of lesions is noticed in freshly cut wound (Figure 8d). Histopathological analysis of the deferoxamine nanoemulgel treated group showed well organized skin architecture with full re-epithelialization, skin adnexal structure repair, and dermal collagen remodeling. There was no evidence of inflammation on the repaired tissue of animals treated with deferoxamine nanoemulgel, indicating that the inflammation had been effectively resolved. The greater wound healing efficacy observed with the deferoxamine nanoemulgel could be due to the prolonged residence time at the wound site, as well as better local delivery and sustained drug release.

Stability Study

Results of the stability study indicate the developed nanoemulgel formulation maintained the original color (white), consistency (homogeneous), drug content (98.27%), spreadability (14.27±0.38 cm) and viscosity (83875±525 cP) when stored at 4°C for 3 months. Furthermore, the drug release profile of nanoemulgel before and after stability study did not differ substantially when evaluated using *t*-test with two samples with equal variances. After three months, the nanoemulgel profile remained comparable and was not statistically significant, as the observed *t*-test value of 0.188 was significantly lower than the t-critical value of 1.76.

CONCLUSION

A systematic study was carried out to develop deferoxamine loaded nanoemulgel for effective wound healing therapy. Initial screening was performed to identify suitable oil, surfactant, and co-surfactant for nanoemulsion preparation by assessing deferoxamine solubility. Oil (oleic acid) and surfactant-co-surfactant (S_{mix}, Tween 80: propylene glycol, 1:3) were used to prepare the nanoemulsion by aqueous titration method. The nanoemulsion was optimized using central composite design, which assessed the impacts of three independent factors (oil quantity, S_{mix}, and water) on key responses (particle size, polydispersity index, and transmittance). The optimized nanoemulsion exhibited desirable characteristics like nano-size droplet, low PDI, high transmittance and good zeta potential. FTIR spectra confirmed compatibility between the drug and formulation components. Morphological evaluation by TEM indicated spherical droplets with uniform dispersion and absence of agglomeration in the prepared nanoemulsion. FTIR spectra confirmed compatibility between the drug and formulation components used, while thermodynamic study confirms stability. The selected nanoemulsion was modified into hydrogel system using carbopol 940 to form nanoemulgel. The developed formulation demonstrated good spreadability, adequate viscosity and no sign of skin irritation, indicating its suitability for skin application. Distinct drug release characteristics were exhibited by nanoemulgel in comparison to control gel, as noticed in the dissimilarity (f_1=50) and similarity (f_2=25) factors. Furthermore, the drug loaded nanoemulgel demonstrated sustained drug release, enhanced skin deposition, and greater improvement in wound contraction. These findings highlight the strong potential of deferoxamine loaded nanoemulgel as a promising topical delivery platform for effective wound healing and support further clinical investigation.

ACKNOWLEDGEMENT

The authors acknowledge the Deanship of Scientific Research, Vice-Presidency for Graduate Studies and Scientific Research, King Faisal University for the support.

ABBREVIATIONS

ANOVA: Analysis of variance; **CCD:** Central composite design; **cP:** Centipoise; **f1:** Dissimilarity factor; **f2:** Similarity factor; **FDA:** Food and Drug Administration; **FTIR:** Fourier transform infrared spectroscopy; **HLB:** Hydrophilic lipophilic balance; **HPLC:** High performance liquid chromatography; **o/w:** Oil in water; **PDI:** Polydispersity index; **R^2:** Coefficient of determination; **SD:** Standard Deviation; **S_{mix}:** Surfactants and Co-Surfactants Mixture; **TEM:** Transmission Electron Microscope.

CONFLICT OF INTEREST

The authors declare that there is no conflict of interest.

FUNDING

This work was supported by the Deanship of Scientific Research, Vice Presidency for Graduate Studies and Scientific Research, King Faisal University, Saudi Arabia [Grant Number KFU263724].

AUTHOR CONTRIBUTION STATEMENT

Conceptualization, ABN, HS, JS; Investigation, ABN, AMA, HS, RMA, ASA; Formal analysis, ABN, AMA, HS, BA, SJ, JS; Methodology, AMA, HS, BA, SJ, RMA, ASA, JS; Funding acquisition, ABN, BA, RMA, ASA; Writing - original draft, AMA, HS, BA, RMA, ASA; Writing - review and editing, ABN, SJ, JS. All authors have contributed significantly to the work, have read, and approved the final manuscript for publication.

SUMMARY

- Deferoxamine-loaded nanoemulgel was successfully developed and optimized via central composite design to enhance topical drug delivery.
- Optimized nanoemulsion exhibited nanoscale droplet size, excellent stability, and uniform morphology.
- Nanoemulgel provided sustained drug release following Korsmeyer-Peppas kinetics and significantly enhanced skin deposition.
- Formulation demonstrated superior physicochemical properties, high drug content, and excellent skin tolerability without irritation.
- *In vivo* studies demonstrated complete wound closure by day 14, along with enhanced tissue regeneration and healing outcomes.

REFERENCES

1. Sen CK. Human Wound and Its Burden: Updated 2025 Compendium of Estimates. Advances in wound care. 2025;14(9):429-438.
2. Peña OA, Martin P. Cellular and molecular mechanisms of skin wound healing. Nature reviews Molecular cell biology. 2024;25(8):599-616.
3. Schilrreff P, Alexiev U. Chronic Inflammation in Non-Healing Skin Wounds and Promising Natural Bioactive Compounds Treatment. International journal of molecular sciences. 2022;23(9).
4. Xu Z, Liang B, Tian J, Wu J. Anti-inflammation biomaterial platforms for chronic wound healing. Biomaterials science. 2021;9(12):4388-4409.
5. Zhao R, Liang H, Clarke E, Jackson C, Xue M. Inflammation in Chronic Wounds. International journal of molecular sciences. 2016;17(12).
6. Raziyeva K, Kim Y, Zharkinbekov Z, Kassymbek K, Jimi S, Saparov A. Immunology of Acute and Chronic Wound Healing. Biomolecules. 2021;11(5).
7. Cano Sanchez M, Lancel S, Boulanger E, Neviere R. Targeting Oxidative Stress and Mitochondrial Dysfunction in the Treatment of Impaired Wound Healing: A Systematic Review. Antioxidants (Basel, Switzerland). 2018;7(8).
8. Beaufay F, Quarles E, Franz A, Katamanin O, Wholey WY, Jakob U. Polyphosphate Functions *in vivo* as an Iron Chelator and Fenton Reaction Inhibitor. mBio. 2020;11(4).
9. Wang G, Yang F, Zhou W, Xiao N, Luo M, Tang Z. The initiation of oxidative stress and therapeutic strategies in wound healing. Biomedicine and pharmacotherapy=Biomedecine and pharmacotherapie. 2023;157:114004.
10. García-Villén F, Souza IMS, de Melo Barbosa R, *et al.* Natural Inorganic Ingredients in Wound Healing. Current pharmaceutical design. 2020;26(6):621-641.
11. Kell DB, Heyden EL, Pretorius E. The Biology of Lactoferrin, an Iron-Binding Protein That Can Help Defend Against Viruses and Bacteria. Frontiers in immunology. 2020;11:1221.
12. Rodrigues M, Bonham CA, Minniti CP, Gupta K, Longaker MT, Gurtner GC. Iron Chelation with Transdermal Deferoxamine Accelerates Healing of Murine Sickle Cell Ulcers. Advances in wound care. 2018;7(10):323-332.
13. Duscher D, Trotsyuk AA, Maan ZN, *et al.* Optimization of transdermal deferoxamine leads to enhanced efficacy in healing skin wounds. Journal of controlled release : official journal of the Controlled Release Society. 2019;308:232-239.
14. Shen H, Ma Y, Qiao Y, Zhang C, Chen J, Zhang R. Application of Deferoxamine in Tissue Regeneration Attributed to Promoted Angiogenesis. Molecules (Basel, Switzerland). 2024;29(9).
15. Lintel H, Abbas DB, Lavin CV, *et al.* Transdermal deferoxamine administration improves excisional wound healing in chronically irradiated murine skin. Journal of translational medicine. 2022;20(1):274.
16. Duscher D, Neofytou E, Wong VW, *et al.* Transdermal deferoxamine prevents pressure-induced diabetic ulcers. Proceedings of the National Academy of Sciences of the United States of America. 2015;112(1):94-99.
17. Chalmers AW, Shammo JM. Evaluation of a new tablet formulation of deferasirox to reduce chronic iron overload after long-term blood transfusions. Therapeutics and clinical risk management. 2016;12:201-208.
18. Berry CE, Abbas DB, Griffin M, *et al.* Deferoxamine topical cream superior to patch in rescuing radiation-induced fibrosis of unwounded and wounded skin. Journal of cellular and molecular medicine. 2024;28(8):e18306.
19. El-Gizawy SA, Nouh A, Saber S, Kira AY. Deferoxamine-loaded transfersomes accelerates healing of pressure ulcers in streptozotocin-induced diabetic rats. Journal of Drug Delivery Science and Technology. 2020;58:101732.
20. Jeckson TA, Neo YP, Sisinthy SP, Foo JB, Choudhury H, Gorain B. Formulation and characterisation of deferoxamine nanofiber as potential wound dressing for the treatment of diabetic foot ulcer. Journal of Drug Delivery Science and Technology. 2021;66:102751.
21. Jacob S, Kather FS, Boddu SHS, Shah J, Nair AB. Innovations in Nanoemulsion Technology: Enhancing Drug Delivery for Oral, Parenteral, and Ophthalmic Applications. Pharmaceutics. 2024;16(10).
22. Nair AB, Kumar S, Dalal P, *et al.* Novel Dermal Delivery Cargos of Clobetasol Propionate: An Update. Pharmaceutics. 2022;14(2).
23. Jacob S, Nair AB. Nanoemulgels as Advanced Topical Drug Delivery Systems: Mechanistic Insights and Therapeutic Applications in Skin Disorders, Infections, Wound Healing, and Cancer. Pharmaceuticals. 2026;19(2):247.
24. Donthi MR, Munnangi SR, Krishna KV, Saha RN, Singhvi G, Dubey SK. Nanoemulgel: A Novel Nano Carrier as a Tool for Topical Drug Delivery. Pharmaceutics. 2023;15(1).
25. Alhazmi HA, ur Rehman Z. A fast and validated chromatographic method for simultaneous determination of deferoxamine and Dpenicillamine via chelate formation with metal ions in bulk and dosage forms. Tropical Journal of Pharmaceutical Research. 2019;18(2):357-364.
26. Nair AB, Chaudhary S, Jacob S, *et al.* Intranasal Administration of Dolutegravir-Loaded Nanoemulsion-Based *in situ* Gel for Enhanced Bioavailability and Direct Brain Targeting. Gels (Basel, Switzerland). 2023;9(2).
27. Nair AB, Singh B, Shah J, *et al.* Formulation and Evaluation of Self-Nanoemulsifying Drug Delivery System Derived Tablet Containing Sertraline. Pharmaceutics. 2022;14(2).
28. Alfehaid FS, Nair AB, Shah H, *et al.* Enhanced transdermal delivery of apremilast loaded ethosomes: Optimization, characterization and *in vivo* evaluation. Journal of Drug Delivery Science and Technology. 2024; 91.
29. Bhanderi M, Shah J, Gorain B, *et al.* Optimized rivastigmine nanoparticles coated with eudragit for intranasal application to brain delivery: evaluation and nasal ciliotoxicity studies. Materials. 2021;14(21):6291.
30. Kotta S, Aldawsari HM, Badr-Eldin SM, Nair AB, Kaleem M, Dalhat MH. Thermosensitive Hydrogels Loaded with Resveratrol Nanoemulsion: Formulation Optimization by Central Composite Design and Evaluation in MCF-7 Human Breast Cancer Cell Lines. Gels (Basel, Switzerland). 2022;8(7).
31. Dantas MG, Reis SA, Damasceno CM, *et al.* Development and Evaluation of Stability of a Gel Formulation Containing the Monoterpene Borneol. TheScientificWorldJournal. 2016; 2016:7394685.
32. Nair A, Gupta R, Vasanti S. *In vitro* controlled release of alfuzosin hydrochloride using HPMC-based matrix tablets and its comparison with marketed product. Pharmaceutical development and technology. 2007;12(6):621-625.
33. Nair AB, Vaka SR, Sammeta SM, *et al.* Trans-ungual iontophoretic delivery of terbinafine. Journal of pharmaceutical sciences. 2009;98(5):1788-1796.
34. Sato H, Ebisawa K, Takanari K, *et al.* Skin-derived precursor cells promote wound healing in diabetic mice. Annals of plastic surgery. 2015;74(1):114-120.
35. Smail SS, Ghareeb MM, Omer HK, Al-Kinani AA, Alany RG. Studies on Surfactants, Cosurfactants, and Oils for Prospective Use in Formulation of Ketorolac Tromethamine Ophthalmic Nanoemulsions. Pharmaceutics. 2021;13(4).
36. Musakhanian J, Osborne DW. Understanding Microemulsions and Nanoemulsions in (Trans)Dermal Delivery. AAPS PharmSciTech. 2025;26(1):31.
37. Pérez-González MLL, González-de la Rosa CH, Pérez-Hernández G, Beltrán HI. Nanostructured oleic acid/polysorbate 80 emulsions with diminished toxicity in NL-20 cell line: Insights of potential drug carriers. Colloids and surfaces B, Biointerfaces. 2020;187:110758.

38. Mirgorodskaya AB, Kushnazarova RA, Lenina OA, Petrov KA, Zakharova LY. Biocompatible Microemulsions Based on Oleic Acid Modified with Piperidinium Surfactants. Russian Journal of General Chemistry. 2023;93(3):593-600.
39. Farag MA, Gad MZ. Omega-9 fatty acids: potential roles in inflammation and cancer management. Journal, genetic engineering and biotechnology. 2022;20(1):48.
40. Chin LY, Tan JYP, Choudhury H, Pandey M, Sisinthy SP, Gorain B. Development and optimization of chitosan coated nanoemulgel of telmisartan for intranasal delivery: A comparative study. Journal of Drug Delivery Science and Technology. 2021;62:102341.
41. Kobra K, Wong SY, Mazumder MAJ, Li X, Arafat MT. Xanthan and gum acacia modified olive oil based nanoemulsion as a controlled delivery vehicle for topical formulations. International journal of biological macromolecules. 2023;253(Pt 4):126868.
42. Szumała P, Kaplińska J, Makurat-Kasprolewicz B, Mania S. Microemulsion Delivery Systems with Low Surfactant Concentrations: Optimization of Structure and Properties by Glycol Cosurfactants. Molecular pharmaceutics. 2023;20(1):232-240.
43. Mistry J, Notman R. Mechanisms of the Drug Penetration Enhancer Propylene Glycol Interacting with Skin Lipid Membranes. The journal of physical chemistry B. 2024;128(16):3885-3897.
44. Kumria R, Nair AB, Al-Dhubiab BE. Loratidine buccal films for allergic rhinitis: development and evaluation. Drug development and industrial pharmacy. 2014;40(5):625-631.
45. Barakoti H, Choudhury A, Dey BK. An outlook for a novel approach: Self-micro emulsifying drug delivery system (SMEDDS). Research Journal of Pharmacy and Technology. 2019;12(4):2055-2064.
46. Ahmad N, Ahmad FJ, Bedi S, Sharma S, Umar S, Ansari MA. A novel Nanoformulation Development of Eugenol and their treatment in inflammation and periodontitis. Saudi pharmaceutical journal : SPJ : the official publication of the Saudi Pharmaceutical Society. 2019;27(6):778-790.
47. Hu M, Xie F, Zhang S, Qi B, Li Y. Effect of nanoemulsion particle size on the bioavailability and bioactivity of perilla oil in rats. Journal of food science. 2021;86(1):206-214.
48. Sarheed O, Dibi M, Ramesh K. Studies on the Effect of Oil and Surfactant on the Formation of Alginate-Based O/W Lidocaine Nanocarriers Using Nanoemulsion Template. Pharmaceutics. 2020;12(12).
49. Che Marzuki NH, Wahab RA, Abdul Hamid M. An overview of nanoemulsion: concepts of development and cosmeceutical applications. Biotechnology and biotechnological equipment. 2019;33(1):779-797.
50. Danaei M, Dehghankhold M, Ataei S, *et al.* Impact of Particle Size and Polydispersity Index on the Clinical Applications of Lipidic Nanocarrier Systems. Pharmaceutics. 2018;10(2).
51. Algahtani MS, Ahmad MZ, Ahmad J. Investigation of Factors Influencing Formation of Nanoemulsion by Spontaneous Emulsification: Impact on Droplet Size, Polydispersity Index, and Stability. Bioengineering (Basel, Switzerland). 2022;9(8).
52. Tarik Alhamdany A, Saeed AMH, Alaayedi M. Nanoemulsion and Solid Nanoemulsion for Improving Oral Delivery of a Breast Cancer Drug: Formulation, Evaluation, and a Comparison Study. Saudi pharmaceutical journal : SPJ : the official publication of the Saudi Pharmaceutical Society. 2021;29(11):1278-1288.
53. Izquierdo P, Feng J, Esquena J, *et al.* The influence of surfactant mixing ratio on nano-emulsion formation by the pit method. Journal of colloid and interface science. 2005;285(1):388-394.
54. Preeti, Sambhakar S, Malik R, *et al.* Nanoemulsion: An Emerging Novel Technology for Improving the Bioavailability of Drugs. Scientifica. 2023;2023:6640103.
55. Da Costa S, Basri M, Shamsudin N, Basri H. Stability of Positively Charged Nanoemulsion Formulation Containing Steroidal Drug for Effective Transdermal Application. Journal of Chemistry. 2014;2014(1):748680.
56. Papandreou P, Triantafyllopoulou E, Pispas I, *et al.* Physicochemical Morphological Evaluation and Stability Assessment of Nanoemulsions Containing Nutrients for Parenteral Nutrition. Colloids and Interfaces. 2025;9(5):64.
57. Rao MR, Aghav S, Sukre G, Kumar M. Determination of required HLB of Capryol 90. Journal of dispersion science and technology. 2014;35(2):161-167.
58. Nair A, Vyas H, Shah J, Kumar A. Effect of permeation enhancers on the iontophoretic transport of metoprolol tartrate and the drug retention in skin. Drug delivery. 2011;18(1):19-25.
59. Ma Q, Zhang J, Lu B, *et al.* Nanoemulgel for Improved Topical Delivery of Desonide: Formulation Design and Characterization. AAPS PharmSciTech. 2021;22(5):163.
60. Alhelal HM, Mehta S, Kadian V, *et al.* Solid Lipid Nanoparticles Embedded Hydrogels as a Promising Carrier for Retarding Irritation of Leflunomide. Gels (Basel, Switzerland). 2023;9(7).
61. Alhasso B, Ghori MU, Rout SP, Conway BR. Development of a Nanoemulgel for the Topical Application of Mupirocin. Pharmaceutics. 2023;15(10).
62. Jacob S, Nair AB. An updated overview with simple and practical approach for developing *in vitro-in vivo* correlation. Drug development research. 2018;79(3):97-110.
63. Milutinov J, Krstonošić V, Ćirin D, Pavlović N. Emulgels: Promising Carrier Systems for Food Ingredients and Drugs. Polymers. 2023;15(10).
64. Ignacyk M, Krasiński Z, Michniak-Kohn B, Cielecka-Piontek J. Innovative Wound Healing Strategy Through Amorphization of Active Pharmaceutical Ingredients as an Effective Approach for Hydrogel Formulation. Pharmaceuticals (Basel, Switzerland). 2025;18(10).
65. Masson-Meyers DS, Andrade TAM, Caetano GF, *et al.* Experimental models and methods for cutaneous wound healing assessment. International journal of experimental pathology. 2020;101(1-2):21-37.

Cite this article: Alotaibi AM, Nair AB, Shah H, Aldhubiab B, Jacob S, *et al*. Deferoxamine Loaded Nanoemulgel for Enhanced Wound Healing: Formulation Optimization and *in vivo* Evaluation. Indian J of Pharmaceutical Education and Research. 2026;60(4s):s1498-s1513.